Soils and Rocks
An International Journal of Geotechnical and Geoenvironmental Engineering
www.soilsandrocks.com
ISSN 1980-9743
ISSN-e 2675-5475

Geomechanical and structural analysis of contaminated residual granitic soils with gasoline

Luis Manuel Ferreira Gomes[1], Gonçalo Teixeira[2], Luis José Andrade Pais[1], Antonio Albuquerque[1], Maria Vitoria Morais[1], André Studart[1], Leonardo Marchiori[1#]

Article

Keywords
Geotechnical characterization
Soil mechanics
Residual soil
Contaminated soils
Gasoline

Abstract
Human activity brings several risks of contamination with pollutants of varying types and effects, with hydrocarbon compounds being of great concern as they are released by vehicles, industrial and construction activities and in areas with fuel reservoirs, among others. Hence, when these contaminants reach the soil, a legitimate question arises regarding their impact on the soil's resistance characteristics. This work presents a case study of granite residual soils contaminated with gasoline under 8-, 16-, and 32-days, within index properties and geomechanical tests were analyzed to support remediation decision. *CBR* tests showed inconsistent results at shallow depths but a 16% capacity reduction beyond 12 mm with green gasoline. Direct shear tests showed similar friction angles but increased cohesion from particle aggregation, raising rupture stress by up to 68%. Oedometer tests showed greater deformability and lower yield stress, with compressibility coefficient around 0.133-0-161, in contaminated soils, aligning with large-deformation *CBR* trends. It seems that gasoline is a complex addition to the soil-water-air interaction, possibly transforming the soil into a hydro-phobic material and thus separating the water as the connecting agent, affecting the overall structure and support capacity of the soil. Future studies should focus on hydrocarbon percolation and leaching behavior in field conditions.

1. Introduction

The growing urbanization increases the demand for land and natural resources, directly impacting civil and geotechnical engineering through extensive earthworks, resource consumption, and waste generation (United Nations, 2020). This expansion often leads to higher waste production and contamination risks, affecting soil, subsoil, and water systems. Carapito (2016) noted that rainwater can leach toxic particles from vehicles—such as heavy metals, hydrocarbons, and tire residues—into the environment.

Pollution reaches soils via gaseous, solid, and liquid emissions from various sources, including industrial discharges, landfills, and fuel-related activities. Despite environmental concerns, sanitary landfills remain the primary disposal method for contaminated waste, risking leakage during structural failures. Hazardous compounds like chlorides, sulfates, nitrates, and hydrocarbons commonly originate from chemical, steel, and thermoelectric industries (Teixeira, 2009). Soil contamination affects not only ecosystems and public health but also infrastructure development, altering soil properties and impeding sustainable growth.

Hydrocarbons, often containing toxic substances like benzene and xylene, pose serious health and environmental risks, with high remediation costs (Hewelke et al., 2018; Roy et al., 2022; Lv et al., 2022). In soil mechanics, fuel contamination alters properties such as structure and permeability, making soils hydrophobic through ion exchange (Andrade Pais, 2007; Hewelke et al., 2018). This affects compressibility, shear strength, and bearing capacity, with lasting changes even after remediation (Mondelli et al., 2010; Braun et al., 2020). Studies show varied geotechnical impacts: Chun et al. (2023) reported that thermal treatment of diesel-contaminated sandy soils enlarged voids and increased hydraulic conductivity due to higher porosity and mean pore linked to enhanced pore connectivity and reduced pore tortuosity. Yazdi & Teshnizi (2021) found that gasoline increased cohesion and consistency in silty soils but decreased friction angle and compaction efficiency over time.

[#]Corresponding author. E-mail address: leonardo.marchiori@ubi.pt
[1]Universidade da Beira Interior, Departamento de Engenharia Civil e Arquitetura, Unidade GeobioSciences, Geotechnologies and GeoEngineering, Covilhã, Portugal.
[2]Proplenitus-Gsft, Unipessoal Lda, Castelo Branco, Portugal

Submitted on July 14, 2025; Final Acceptance on November 3, 2025; Discussion open until November 30, 2026.
Editor: Renato P. Cunha
https://doi.org/10.28927/SR.2026.009225

Several remediation methods have proven effective: biofertilizers and activated alloys removed up to 22% oil (Akhanova et al., 2023); microbial methods achieved up to 52% degradation (Zhao et al., 2011). Advanced solutions include nanotechnologies, thermal desorption, and electrochemical and oxidation processes (Cheng et al., 2016; Ambaye et al., 2022). Hydrocarbon exposure also poses health risks, with Roy et al. (2022) highlighting elevated cancer risks in road and traffic areas. Given current pollution levels, it is vital to assess how hydrocarbons affect soil mechanics, which depend on granulometry, particle structure, mineralogy, and geological history (Terzaghi & Peck, 1948; Gomes, 1986; Teixeira, 2009).

This study investigates a granite residual soil from Covilhã (Castelo Branco, Portugal), shaped by erosive geological processes and derived from granitic lithology rich in quartz with a silt-clay matrix mainly composed of kaolinite (Cunha, 1987; Dias, 1998; Marchiori et al., 2021, 2022). Formed by granite weathering and tectonism, these residual soils are typically sandy and suitable for earthworks. However, their degree of alteration varies, influencing physicochemical properties (Andrade Pais, 2007). Gasoline-soil interactions are complex, as hydrophobic compounds, hydrocarbons disrupt the soil-air-water balance, potentially creating air pockets and affecting mechanical behavior. Capillary tension and creep also influence physical indices like water content and dry density (Andrade Pais, 2007).

The research aims to compare the geotechnical properties of uncontaminated and green gasoline-contaminated residual granite soils, assessing how contamination affects mechanical behavior, alters soil structure, and to interpretate due to its variability and deviation from typical soil characteristics.

2. Materials and methods

The analyzed granite residual soil was obtained in Covilhã, Portugal, by collecting 7 undisturbed samples at different depths, along a 5.80 m depth vertical slope, as Figure 1a summarizes. In situ tests were carried out to obtain the particle volume weight (γ_d), natural moisture content (w_N) and initial void index (e_0). In the laboratory, the samples were subjected to natural drying and crushing, where the homogenization of individual samples *S1* to *S7* was carried out into a single global sample of the massif (*St*). Then, particle size distribution, Atterberg limits and volumetric weight of solid particles were carried out for samples *S1* to *S7* and *St*, following the standards in Table 1. In a second phase, with only the *St* sample, the material was sieved in 4.75 mm mesh, to avoid including larger material, promoting better homogenization and workability. This sample was used to carry out Proctor compaction with small and large molds, combining Normal and Modified energy, *CBR* test, direct shear, and consolidation oedometric tests.

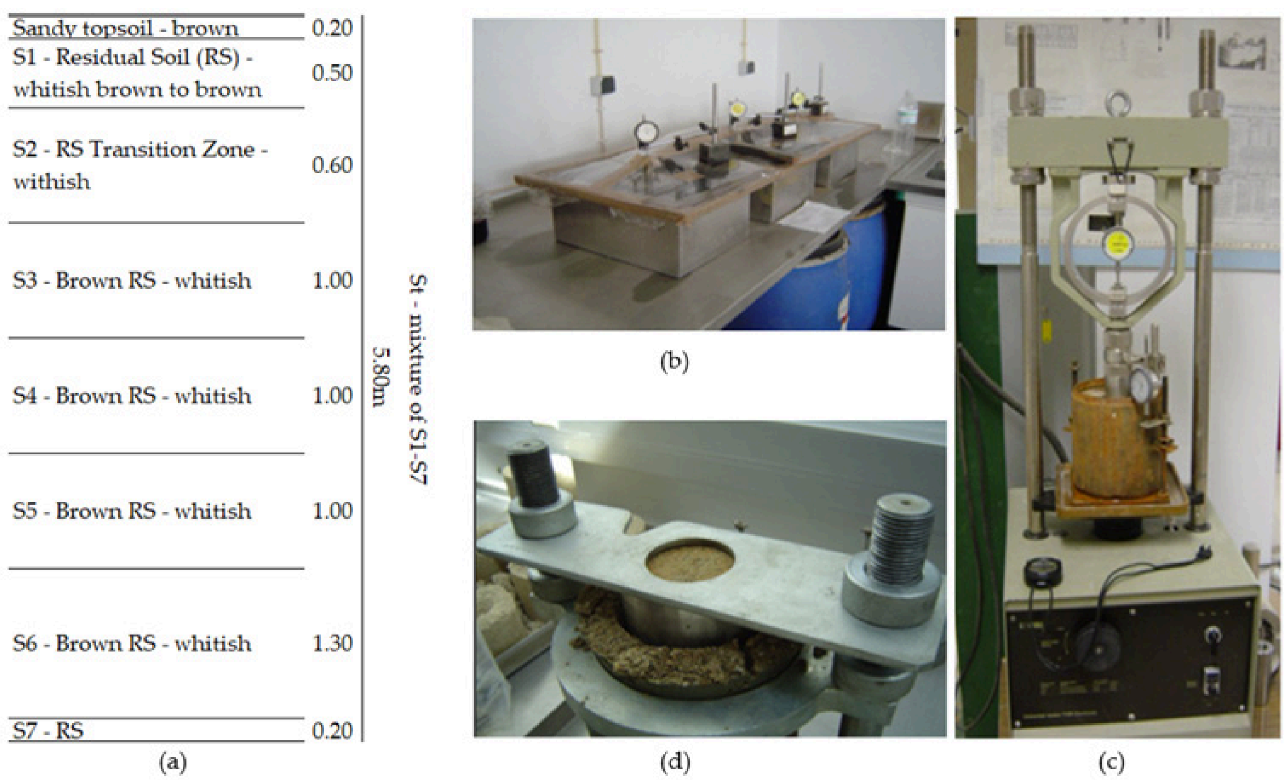

Figure 1. Sampling and testing: (a) sample's collection depths, (b) immersion phase of the specimens (c) CBR test, and (d) sample extraction through CBR mold.

Proctor tests were carried out in small (SM) and large molds (LM), with normal (NE) - 6kg /cm^2 - and modified (ME) – 27 kg/cm^2 - energies associated to each mold for better understanding on the compaction scales of the soil, using St sample. Samples were then prepared for *CBR*, based on the LM (NE) optimal parameters, according to Table 2. All samples were submerged in water during 8, 16, and 32 days and were compacted in 3 different water contents, with the optimal, minus 3%, and plus 3%. For the submerged with gasoline, only optimal water content was considered while 8, 16, and 32 days of immersion were maintained in comparison with different compaction states of the soil.

All tested specimens were in cylindrical shape. The specimens associated with the large mold were immersed in distilled water, while Wopt specimens were also immersed in the contaminant (green gasoline). All specimens were subjected to *CBR* tests after 8-, 16-, and 32-days of immersion, having been made 12 tests each immersion time. Then, from the various specimens subjected by *CBR* tests, the affected soil was removed from the top, and specimens for direct shear and oedometric test were extracted from *CBR* mold using special rings. Figures 1b-d shows the immersion, the test, and extraction phase of the analyzed samples. *CBR* Type used a 5 cm^2 piston with a displacement of 1 mm/min.

For direct shear, the equipment by Control was used, carried out using a dynamometric ring with a capacity of 2 kN at a speed of 0.6 mm/min. The tested specimens have a 10.0 cm diameter, with a height of 2.5 cm. Regarding the direct shear, the specimens were tested soaked in distilled water, with a shear rate of 0.05%/mm to ensure drainage during shearing. The oedometric test was carried out using equipment by ELE, with a deflectometer with an accuracy of 0.002 mm and circular specimens with a diameter and height of 6.3 cm and 2 cm, respectively. The loads and unloads were applied and scaled following 9 – 41 – 81 – 160 – 319 – 636 – 1271 – 2541 – 41 kPa, respecting 24 h of time for each stage, with a reading carried out on a logarithmic scale. The one-stage unload was done due to the low swelling prediction according to the soil's index properties, providing a linear phase for the coefficient of swell determination.

Table 1. Conducted tests according to the standards.

Type of test	Standard or procedure
In situ sampling	ASTM D420-18 (ASTM, 2018)
Particle size distribution	ASTM D6913/D6913M (ASTM, 2021b)
Atterberg limits	ISO 17892-12 (ISO, 2018a, b, c, 2019)
Proctor compaction	ASTM D698-12 (ASTM, 2021c)
CBR type	ASTM D1883 (ASTM, 2021a)
Direct shear	ASTM D3080-04 (ASTM, 2004)
Oedometric consolidation	ISO 17892-5 (ISO, 2017)

3. Analysis and results

The experiments sought to characterize the original soil and after contamination with gasoline to allow evaluation of the impacts of the contaminant on the micro and macrostructure of the soil, as well as in its classification, granulometry, density and Atterberg limits, compaction parameters (represented by Proctor) and resistance (represented by *CBR* and direct shear).

3.1 Sampling and physical identification

The results of the in situ parameters from sampling depths (Figure 1a), and dry volumetric weight (γ_d), water content (w_N) and void index (e_0), are presented in Table 3. The γ_d values vary between 16.2 and 17.4 kN/m3, being the lowest value correspondent to the most superficial soil and the highest for the maximum test depth. This pattern was also seen in e_0, with values between 0.623 and 0.543, showing greater densification of natural materials at greater depths. The w_N values average 12.5%, although there is a tendency for higher values to occur close to the surface and lower values for greater test depths. Besides, the particle size distributions of the samples are shown in Figure 2. Table 3 also presents laboratorial results for the clay, silt, and sand

Table 2. Tested samples nomenclatures and explanations.

Sample Nomenclature	Embedded Fluid (-)	Compaction moisture (%)	Immersion (days)
Wopt (8)	(W) Water	(opt) Optimal	8
Wopt+3% (8)	(W) Water	(opt+3%) Optimal + 3%	8
Wopt-3% (8)	(W) Water	(opt-3%) Optimal - 3%	8
WoptG (8)	(G) Gasoline	(opt) Optimal	8
Wopt (16)	(W) Water	(opt) Optimal	16
Wopt+3% (16)	(W) Water	(opt+3%) Optimal + 3%	16
Wopt-3% (16)	(W) Water	(opt-3%) Optimal - 3%	16
WoptG (16)	(G) Gasoline	(opt) Optimal	16
Wopt (32)	(W) Water	(opt) Optimal	32
Wopt+3% (32)	(W) Water	(opt+3%) Optimal + 3%	32
Wopt-3% (32)	(W) Water	(opt-3%) Optimal - 3%	32
WoptG (32)	(G) Gasoline	(opt) Optimal	32
Wopt (8)	(W) Water	(opt) Optimal	8

Table 3. Sampling in situ characteristics.

Sample (average depth)	γ_d (kN/m³)	w_N (%)	e_0 (-)	Clay (%)	Silt (%)	Sand (%)	C_U (-)	C_C (-)	w_L (%)	w_P (%)	*PI* (%)	γ_s (kN/m³)	USCS (-)	AASHTO (-)
S1 (0.45m)	16.2	11.8	0.623	5	17	58	114	1.8	24	22	2	25.8	SW-SM	A-2-4 (0)
S2 (1.00m)	16.7	15.6	0.593	4	15	53	133	3.0	35	32	3	26.1	SW-SM	A-1-b (0)
S3 (1.80m)	16.9	14.6	0.580	3	14	54	100	2.0	29	27	2	26.2	SW-SM	A-1-b (0)
S4 (2.80m)	17.0	11.5	0.576	4	10	51	75	2.1	33	30	3	26.3	SW-SM	A-1-b (0)
S5 (3.80m)	17.2	11.5	0.564	3	12	45	80	1.8	34	31	3	26.4	SW-SM	A-1-b (0)
S6 (4.95m)	17.4	11.8	0.546	2	11	47	80	2.7	30	27	3	26.4	SW-SM	A-1-b (0)
S7 (5.70m)	17.5	9.9	0.543	2	8	42	42	2.4	32	30	2	26.5	SW-SM	A-1-b (0)
St	-	-	-	4	12	43	105	2.9	31	28	3	26.2	SW-SM	A-1-b (0)

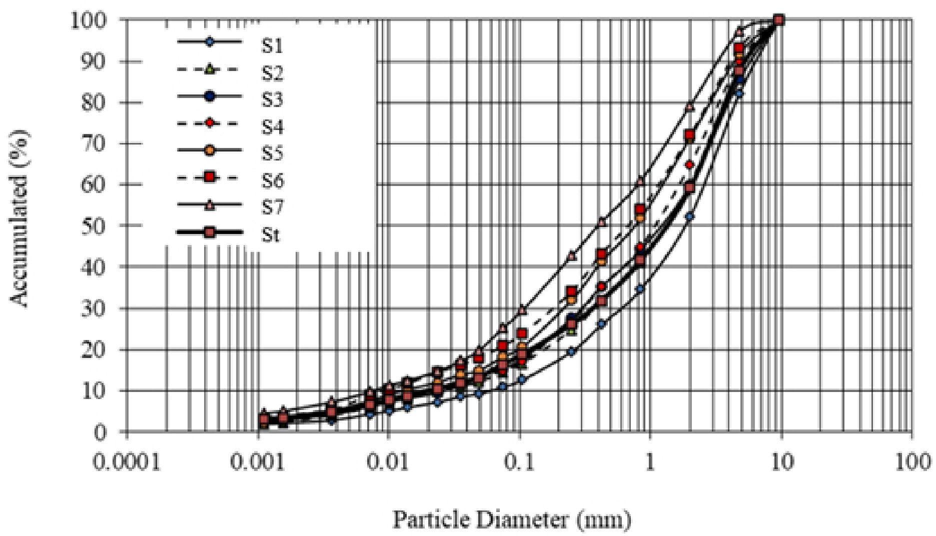

Figure 2. Particle size distributions.

fractions of the various samples, as well as the respective uniformity (C_U) and curvature (C_C) coefficients, Atterberg limits, grain volume weight (γ_s) and soil classifications according to USCS and AASHTO.

It is possible to indicate that the analyzed samples have a high amount of sand, ranging from 42% to 58%, with a low clay content, reaching a maximum value of 5%, indicating the susceptibility of this type of soil to construction in general, corresponding to a granular material of great to excellent quality for sub-grade, based on AASHTO, and a well graded silty sand (SW-SM) based on the USCS.

The values of γ_s indicate densities with particle values of granitic origins, corroborating with the material analyzed here. Andrade Pais (2007) indicates that there is the presence of coarse-grained porphyroids granite in the Covilhã region, where the alteration of the granite occurs through the transformation of associated feldspars into clayey materials, namely kaolinite, being a clay group generally associated with low plasticity, corroborating with the found plasticity index (*PI*) values. However, given that the clay content in the samples is relatively small (<5%), it is likely that the overall low plasticity is also strongly influenced by the higher proportion of silt (8–17%), which behaves as a plastic fraction and dilutes the clay's contribution to the Atterberg limits. Furthermore, considering that the *PI* is characterized as low, this can be considered a desirable characteristic for the use of the material in various applications in civil engineering.

The Proctor compaction was carried out in SM and LM, with light (NE) and heavy (ME) energy associated with each mold. Figure 3 shows Proctor compaction curves. The results obtained show that with greater energy, a higher level of compactness is achieved, requiring less water for hydration and union of the particles, as expected. Furthermore, the values indicate an optimal water content of approximately 13% for Normal energy and 9% for Modified. Lower water content is expected for sandy soils, since the larger the particle size, the smaller its specific surface will be, due to the greater mass per unit area (Takei, 2019), requiring a lower water content for optimal hydration. With higher compaction energy, compaction is carried out more efficiently, the soil tends to become more compressed and with a greater connection between the particles, reducing the voids in the soil structure, and, therefore, requiring less water to reach their optimal moisture content.

Figure 3 also presents the results in terms of maximum dry volumetric weight (γ_{dmax}) and respective optimum moisture content (*OMC*) for different types of compaction and energies. According to the results obtained, the large mold was considered the most representative mold for sampling, as it allows a greater representative quantity of material with considerable homogenization. Furthermore, *NE* is considered more representative as it presents greater difficulty in obtaining optimal compaction, representing a closer approach to in-nature cases, while allowing fluids' percolation, such as water and gasoline. This combination was used for *CBR* Type, direct shear and oedometric tests.

3.2 Geomechanics characteristics

3.2.1 CBR

The load vs. displacement for the *CBR* Type tests are shown in Figure 4, organized by the three immersion periods of 8-, 16- and 32-days. It should be noted that each of the curves presented resulted from the average of the values obtained in replicated tests.

The higher the contact time of the soil with the immersion fluid, distilled water, or contaminant (gasoline),

Parameter	LM (NE)	SM (NE)	LM (ME)	SM (ME)
γ_{dmax} (kN/m^3)	18.6	18.7	20.1	19.9
OMC (%)	13.1	13.4	9.1	9.5

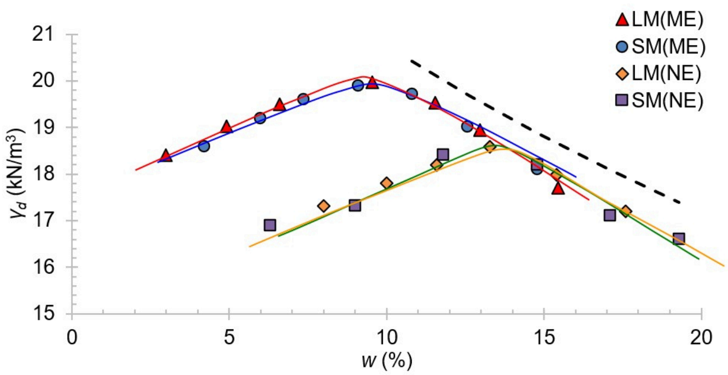

Figure 3. Proctor compaction curves and optimal parameters.

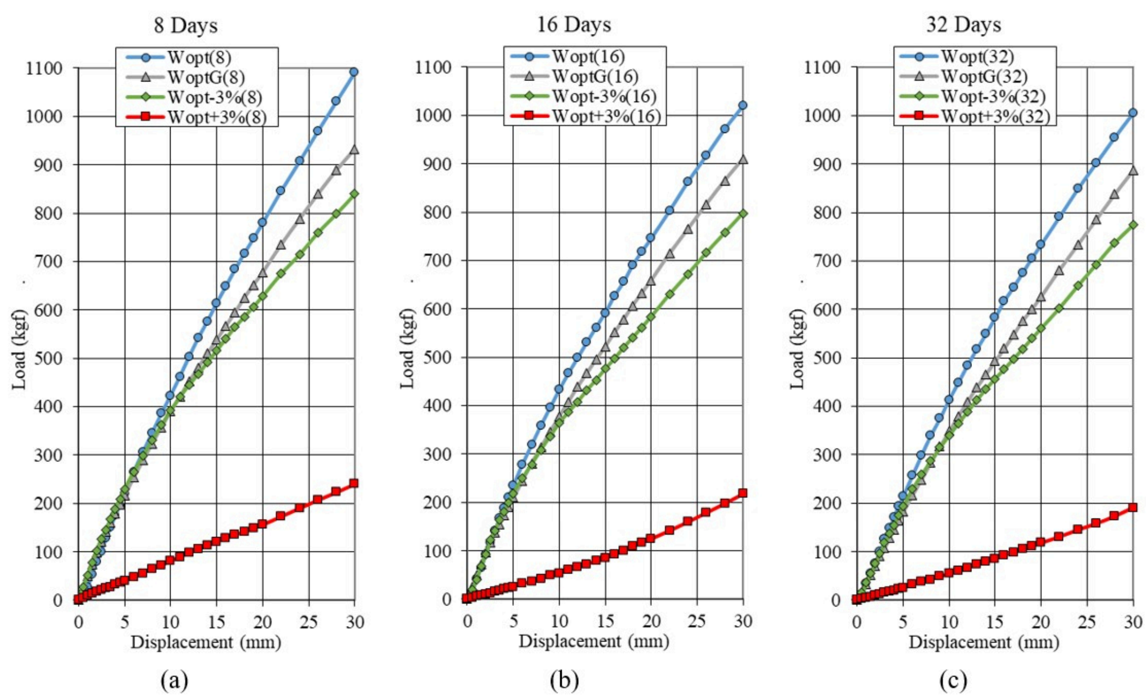

Figure 4. *CBR* tests in specimens with immersion of: (a) 8 days, (b) 16 days, and (c) 32 days.

a slight reduction in support capacity is seen for the same displacement. It was evident and consistent across all immersion groups that there was a sequence of load support, ranging from the lowest to the highest, based on the samples: Wopt+3% < Wopt-3% < WoptG < Wopt. This indicates that the specimens with the lowest resistance are those that were compacted with a water content above 3% in relation to the optimum, and the specimens compacted with the optimum water content without contaminants were always the most resistant.

It is worth noting that gasoline's immersion reduced the soil's support capacity by up to 16%, probably due to the lubricating effect, creating a more susceptible sliding plane and therefore impairing the obstruction between particles. However, such differences are only noticeable after 12mm of penetration since the load prior to this penetration is not high enough to distinguish the materials. Considering the piston of the *CBR* test as if it was a plate, similarly to a plate load test, the results for all specimens in terms of stress vs. displacement curves are presented in Figure 5. The curves corresponding to the situation of the specimens Wopt+3% had a clear punching behavior for all the immersion times, while the other curves present an evolution of the localized failure type corresponding to soils of medium to lower compactness.

3.2.2 Direct shear

In addition to road applications, residual granite soils are generally considered good earthwork materials suitable for several applications. Therefore, it is necessary to evaluate the shear strength and obtain values of internal friction angle and cohesion, which allow the analysis of the impact of contaminating agents on mechanical resistance.

Direct shear tests were carried out on specimens obtained from compaction tests, as abovementioned. It is noted that there was some difficulty in making the samples, particularly in the samples compacted with Wopt-3%, as the soil was very dry and a little "brittle". Figures 6a and 6b presents a comparison of shear stress by horizontal displacement, while Figure 6c and 6d presents horizontal displacements by vertical displacements and Figure 6e and 6f presents the rupture envelopes between the soil and the contaminated soil for 16 days, as it was the mean tested time.

Table 4 presents the parameters of shear resistance, internal friction angle (ϕ) and cohesion (c), obtained from the maximum stresses, of all direct shear tests carried out. The values found for ϕ demonstrate a variability between 31.1 and 37.2°, and from 10.1 to 37.6 kPa for cohesion. In the specimens with identical compaction at optimal, and immersion fluids, the variation in ϕ can be considered insignificant since it changes less than 2% for the 8-days immersion, the 16-days remains the same value, and for the 32-days, less than 3% change. However, the same does not happen with cohesion, where there is a drastic increase when in contact with the green gasoline contaminant, demonstrating the impact of gasoline on the agglomeration of soil particles, functioning as a binding agent. Those results are probably due to the lubricating effect of the quartz grains, which are very rough. Their friction is very significant in situations of longer immersion time, as agglutination of fine particles takes place in contaminated samples.

3.2.3 Structural analysis

To make a comparison of the results of the *CBR* Type test presented previously as plate load test in Figure 6, the applied stress analysis continued as a footing equivalent to the circular plate of diameter B, corresponding to the *CBR* test piston. Continuing then, applying Equation 1, which

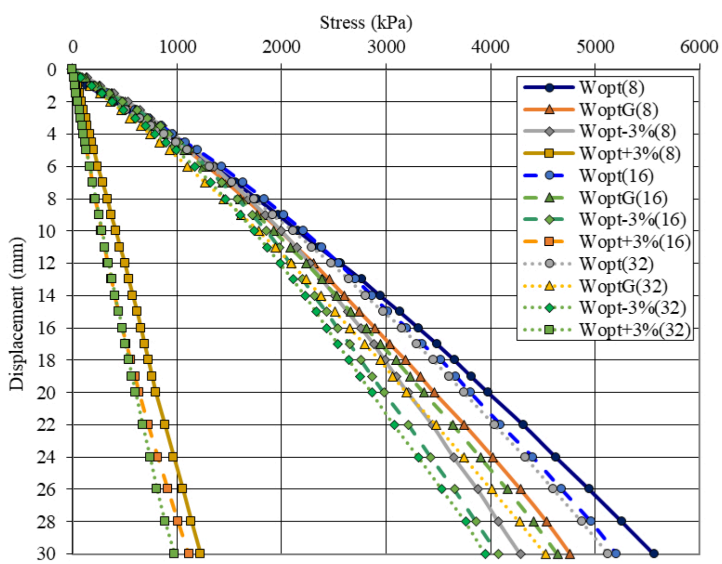

Figure 5. Stress vs. displacement interpretation as plate load test.

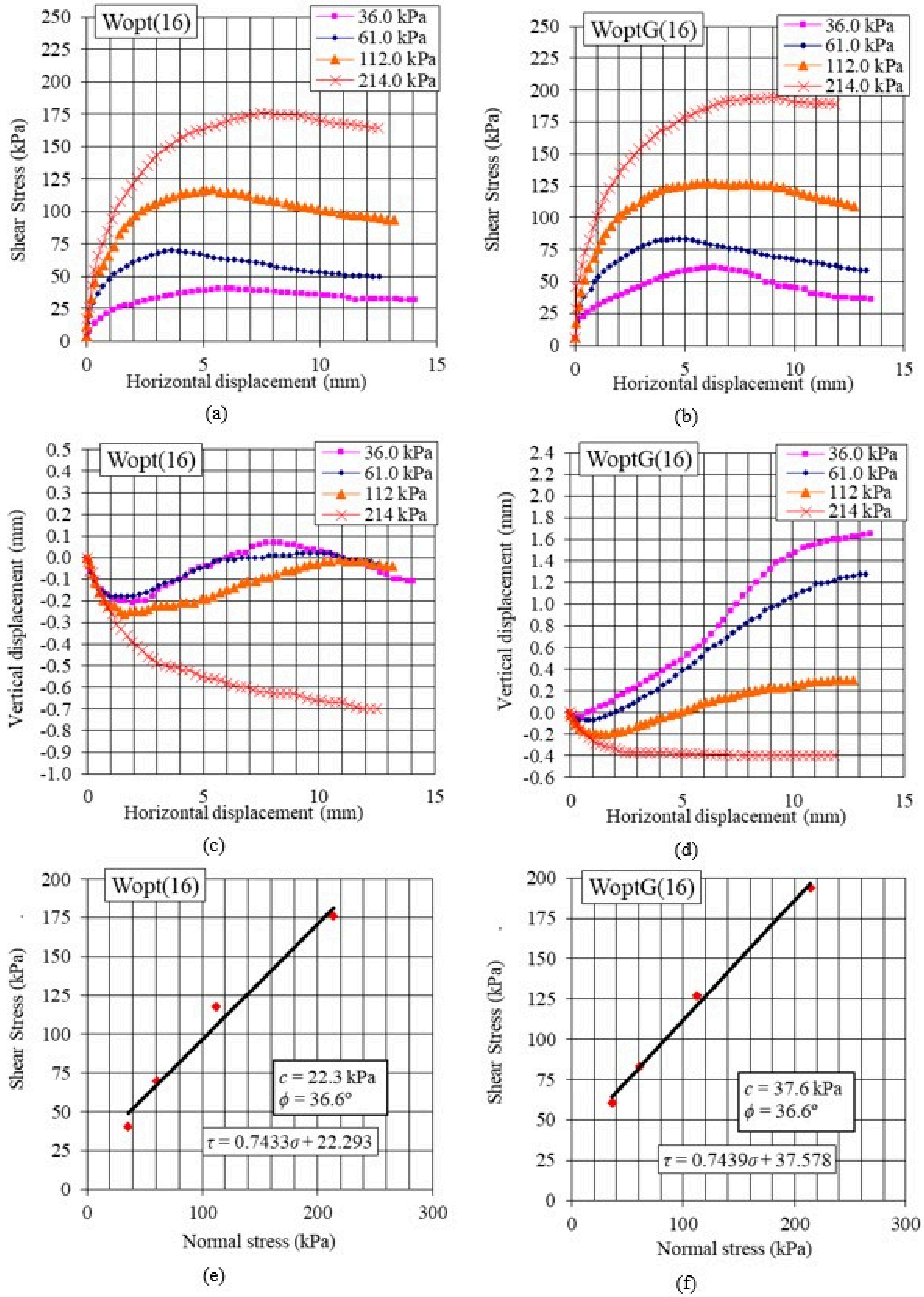

Figure 6. Shear stress vs. horizontal displacement for: (a) 16-days immersion for soil in distilled water, and (b) gasoline, (c) vertical vs. horizontal displacement for 16-days immersion for soil in distilled water, and (d) gasoline, (e) envelope curves for 16-days immersion for soil in distilled water, and (f) gasoline.

Table 4. Direct shear results.

Sample	Wopt (8)	WoptG (8)	Wopt-3% (8)	Wopt+3% (8)
ϕ (°)	36.8	36.0	31.1	35.6
c (kPa)	18.1	30.7	18.7	10.1
Sample	Wopt (16)	WoptG (16)	Wopt-3% (16)	Wopt+3% (16)
ϕ (°)	36.6	36.6	33.1	35.6
c (kPa)	22.3	37.6	17.5	18.9
Sample	Wopt (32)	WoptG (32)	Wopt-3% (32)	Wopt+3% (32)
ϕ (°)	35.6	36.6	37.2	36.1
c (kPa)	25.0	36.8	12.6	22.2

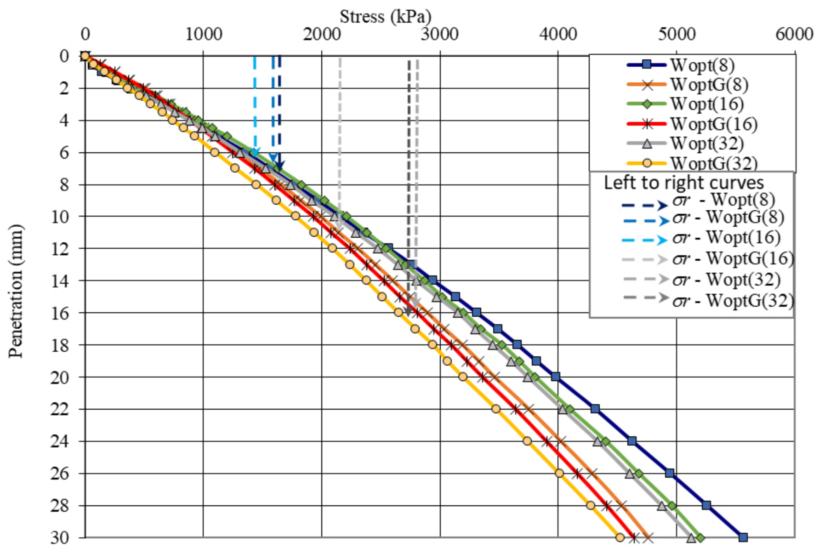

Figure 7. Comparison between *CBR* and structural analysis for optimal samples.

refers to the classic load capacity equation applied to direct foundations, using the parameters obtained in the direct shear test, based on (Terzaghi & Peck, 1948).

$$\sigma_r = c \cdot \delta_c \cdot N_c + q \cdot \delta_q \cdot N_q + 0.5 \cdot \gamma_B \cdot B \cdot \delta_\gamma \cdot N_\gamma \quad (1)$$

where σ_r is the rupture stress composed of three parts, the first referring to the cohesion, where c is soil's cohesion; the second to the overload, where q is the effective vertical tension at the level of the loaded base; and the third to the base, where γB refers to the volumetric weight of the soil below the base of the loaded area and B the width or diameter of the loaded base besides. N_c, N_q and N_γ are the load capacity factors, which depend only on the friction angle, the factors δ_c, δ_q and δ_γ are shape factors dependents of the geometry of the foundation area, considered as circular.

Optimal conditions with and without green gasoline were considered for all samples to verify the maximum resistance. For the calculation, q value was considered as zero as it is equivalent to a surface load where the depth is zero, to simulate *CBR* test, where the loading is on the surface of the specimen; γ_B of 21.2 kN/m^3 is used, which is the value corresponding to the volumetric weight for the optimal situation, but saturated. The values of δ_c, δ_q and δ_γ while N_c, N_q and N_γ correspond to the values calculated from the internal friction angle, with based on Terzaghi and Peck's proposal. Calculated parameters exposed in Figure 7.

According to the results shown for σ_r, the load capacity increases in contaminated soils between 52 and 68%. This effect is the fundamental result of the increase in the cohesion of these soils because of contamination by green gasoline. In comparison with the results obtained in the *CBR* test, it appears that the order of magnitude of σ_r' corresponds to penetrations between 6 and 16mm. The apparent contradiction between the structural analysis and the *CBR* tests is justified due to the tensions used, where in the *CBR* the specimens with low penetrations were also shown to have a higher support capacity when contaminated with gasoline. Figure 7 and Table 5 aim to correlate the results found between the structural analysis, represented by the dotted lines, and the results of the *CBR*, with the curves previously presented.

Therefore, the unpredictability of soil behavior when contaminated is highlighted, since gasoline has binding and lubricating characteristics, and will impact the soil structure depending on the load. *CBR* test has exposed that the resistant stress values found for contaminated soils are considerably lower compared to uncontaminated soils, when at high stresses.

3.2.4 Oedometric consolidation

Considering the characterization regarding particle size and resistance capacity, it is necessary to obtain consolidation parameters. The consolidation curves for 8-, 16- and 32-days immersion are presented in Figure 8, standardized by the void index (e/e_0) vs. effective vertical stress (σ_v'). The results regarding oedometric tests in Table 6 exposes compression (C_c) and swelling index (C_s), besides structural yield stress (σ_{vm}') for all the materials involved.

It was concluded that contaminated soils have slightly greater compressibility than uncontaminated soils, when comparing the results of samples compacted at *OMC*. Contaminated soils showed lower structural yield stress, in accordance with the oedometer results, where greater stresses lowered the resistance of contaminated soils. The lubricating effect of gasoline appears to have a direct effect on the reorganization of particles and can make them more compressible, resulting in a clayey behavior, where the presence of fluids reduces resistance to compression.

Table 5. *CBR* and structural analysis for optimal samples results.

Sample	Wopt (8)	WoptG (8)	Wopt (16)	WoptG (16)	Wopt (32)	WoptG (32)
ϕ (°)	36.8	36.0	36.6	36.6	35.6	36.6
c (kPa)	18.1	30.7	22.3	37.6	25.0	36.8
N_c (-)	56.0	50.6	53.0	53.0	48.3	53.0
δ_c (-)	1.3	1.3	1.3	1.3	1.3	1.3
q (kPa)	0	0	0	0	0	0
δ_q (-)	1.2	1.2	1.2	1.2	1.2	1.2
γ_B (kN/m^3)	21.2	21.2	21.2	21.2	21.2	21.2
B (m)	0.05	0.05	0.05	0.05	0.05	0.05
N_γ (-)	53.0	40.0	52.8	52.8	38.5	52.8
δ_γ (-)	0.6	0.6	0.6	0.6	0.6	0.6
σ_r (kPa)	1334.53	2032.17	1552.68	2606.45	1580.37	2551.35

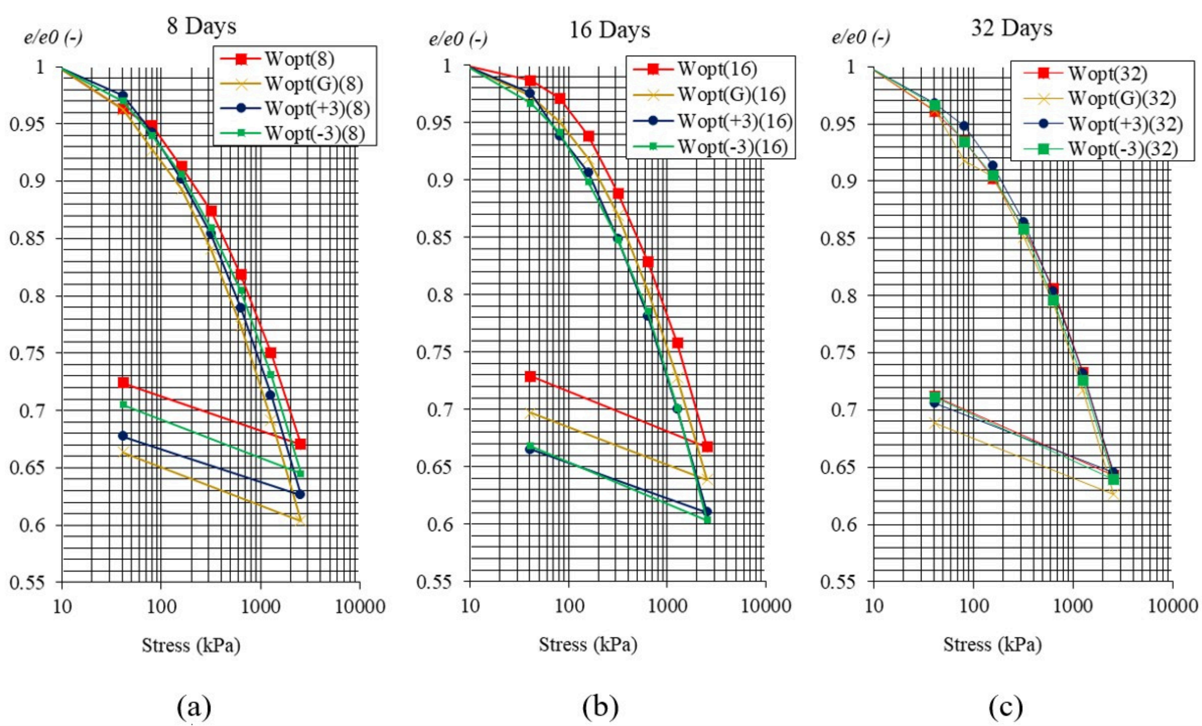

Figure 8. Oedometric consolidation curves for 8- (a), 16- (b) and 32-days (c) immersion.

Table 6. Oedometric consolidation results.

Sample	C_c (-)	C_s (-)	σ'_{vm} (kPa)
Wopt (8)	0.133	0.016	300
WoptG (8)	0.151	0.018	220
Wopt – 3% (8)	0.153	0.018	320
Wopt + 3% (8)	0.159	0.016	250
Wopt (16)	0.140	0.018	295
WoptG (16)	0.151	0.018	280
Wopt – 3% (16)	0.154	0.018	285
Wopt + 3 (16)	0.161	0.017	220
Wopt (32)	0.133	0.019	350
WoptG (32)	0.150	0.018	295
Wopt - 3% (32)	0.136	0.019	360
Wopt + 3% (32)	0.133	0.016	320

4. Discussion

Residual soils result from rock weathering; in igneous rocks, uplift and exposure to wind or water transform rock masses into soil—a complex, variable process (Duarte, 2002). Depending on weathering intensity, these soils range in grain size from clay to gravel (Viana da Fonseca, 2005) and inherit mineralogical traits from the parent rock. In Covilhã, granite-derived soils are rich in quartz and feldspar, with a kaolinite matrix from feldspar alteration (Andrade Pais, 2007), influencing compressibility and strength.

Mineralogy directly affects soil behavior. Compression index values for granitic soils range from 0.05 to 0.52 (Adebisi & Adeyemi, 2012), with Portuguese granite soils typically between 0.10 and 0.27 (Duarte, 2002; Andrade Pais, 2007). Contaminants alter particle bonding and suction, reducing compressibility and introducing variability over time due to creep (Karkush et al., 2013). Friction angles typically range from 29°–36° (Lemos & Andrade Pais, 2000; Duarte, 2002), while cohesion increases significantly in gasoline-contaminated soils—from 1.3 to 9.2 kPa up to 50 kPa (Barik, 2010; ASRTE, 2010; Duarte, 2002).

Gasoline's hydrophobicity alters interparticle forces, causing fine particles to agglomerate into larger clusters. This apparent coarsening effect increases the sand fraction and modifies soil structure, thereby influencing compaction, strength, and hydraulic behavior. (Andrade Pais & Ferreira-Gomes, 2012). Therefore, *CBR* tests show a 16% support loss due to lubrication and sliding, while low-stress structural analysis suggests increased bearing capacity—an effect that diminishes at higher stress levels.

Hydrocarbons increase pore pressure, reduce resistance, intensify lubrication effects, directly impacting cohesion and strength (Yazdi & Teshnizi, 2021). These effects vary with exposure time, hydrocarbon type, and contamination level, making mechanical behavior less predictable. Beyond geotechnics, hydrocarbon contamination threatens aquifers and food chains, demanding costly remediation (Zhang et al., 2014; Ossai et al., 2020; Rodrigo-Ilarri et al., 2023).

5. Conclusion

This study assessed granite residual soils, compacted with and without green gasoline contamination under different immersion periods. The main findings are that *CBR* tests showed unclear effects for small penetrations, but from 12 mm onward, green gasoline reduc ed capacity by 16%; direct shear tests indicated little change in friction angle, but a notable increase in cohesion in contaminated samples, likely due to particle aggregation acting as a binder; rupture stress increased by up to 68% in contaminated soils, attributed to higher cohesion. Although structural analysis and *CBR* tests appear contradictory, *CBR* also showed higher capacity at shallow depths when contaminated; oedometer tests revealed contaminated soils are slightly more deformable and exhibit lower yield stress, aligning with large-deformation *CBR* results. Effects depend on exposure time, contaminant volume, and fuel chemistry. Long-term exposure is expected to weaken structure and reduce support capacity, while also posing environmental risks.

Laboratory immersion and compaction procedures may not entirely replicate complex field conditions, such as fluctuating groundwater levels, heterogeneous soil layering, variable contamination volumes, and long-term environmental exposure. The study is also limited by the focus on a single type of residual granite soil and one contaminant, which restricts generalizability to other soil types or hydrocarbon mixtures. Additionally, the observed effects were measured over relatively short immersion durations, limiting insights into long-term mechanical and environmental impacts. Future research should pursue field-scale investigations to validate laboratory findings and account for natural hydrogeological variability. Extended studies on the percolation, aging, and leaching behavior of gasoline and its byproducts under real environmental cycles are crucial. Moreover, work should encompass various soil and contaminant types, especially investigating chronic, low-level exposures and their influence on remediation efficacy and soil structure resilience.

Acknowledgments

The authors acknowledge the support by the GeoBioTec Research Unit through the strategic projects UIDB/04035/2025 (https://doi.org/10.54499/UIDB/04035/2020) and UIDP/04035/2020 (https://doi.org/10.54499/UIDP/04035/2020), from Fundação para a Ciência e a Tecnologia (FCT).

Declaration of interest

The authors have no conflicts of interest to declare. All co-authors have observed and affirmed the contents of the paper and there is no financial interest to report.

Authors' contributions

Luis Manuel Ferreira Gomes: conceptualization, data curation, visualization, writing – original draft, resources. Gonçalo Teixeira: conceptualization, data curation, methodology, validation, writing – original draft. Luis José Andrade Pais: formal analysis, investigation, methodology, project administration, resources. Antonio Albuquerque: supervision, funding acquisition, investigation validation, writing – review and editing. Maria Vitoria Morais: data curation, validation, writing – review and editing. André Studart: data curation, validation, writing – review and editing. Leonardo Marchiori: supervision, data curation, validation, writing – original draft, review and editing.

Data availability

All data produced or examined in the course of the current study are included in this article.

Declaration of use of generative artificial intelligence

This work was prepared without the assistance of any generative artificial intelligence (GenAI) tools or services. All aspects of the manuscript were developed solely by the authors, who take full responsibility for the content of this publication.

List of symbols and abbreviations

c	Cohesion
e	Void index
e_0	Initial void index
q	Effective vertical tension
w_L	Liquid limit
w_N	Natural moisture content
w_P	Plastic limit
AASTHO	American Association of State Highway and Transportation Officials
ASTM	American Society for Testing and Materials
B	Diameter of circular plate
CBR	California Bearing Ratio
C_C	Curvature coefficient
C_c	Compression index
C_s	Swelling index
C_U	Uniformity coefficient
ELE	ELE International
G	Gasoline
GeoBioTec	Geobiosciences, Geoengineering and Geotechnologies
ISO	International Organization for Standardization
LM	Large mold
ME	Modified energy
N_c	Load capacity factor for cohesion
N_q	Load capacity factor for effective vertical tension
N_γ	Load capacity factor for volumetric weight
NE	Normal energy
OMC	Optimal moisture content
PI	Plastic index
RS	Residual soil
S1-7	Sample 1 to sample 7
SM	Small mold
St	Global sample of the massif
USCS	Unified Soil Classification System
W	Water
δ_c	Shape factor for cohesion
δ_q	Shape factor for effective vertical tension
δ_γ	Shape factor for volumetric weight
ϕ	Internal friction angle
γ_B	Volumetric weight
γ_d	Particle volume weight
γ_{dmax}	Maximum dry volumetric weight
γ_s	Grain volume weight
σ_r	Rupture stress
σ_v'	Effective vertical stress
σ_{vm}'	Structural yield stress

References

Adebisi, N., & Adeyemi, G. (2012). Assessment of compressibility characteristics of residual laterised soils in southwestern Nigeria. *Science Focus*, 17(2), 198-208.

Akhanova, T., Lyubchenko, N., Sarmurzina, R., Karabalin, U., Muhr, H., & Boiko, G. (2023). Complex restoration of oil contaminated soils with new organomineral reagents. *Water, Air, and Soil Pollution*, 234(11), 685-702. https://doi.org/10.1007/s11270-023-06689-8.

Ambaye, T., Chebbi, A., Formicola, F., Prasad, S., Gomez, F., Franzetti, A., & Vaccari, M. (2022). Remediation of soil polluted with petroleum hydrocarbons and its reuse for agriculture: recent progress, challenges, and perspectives. *Chemosphere*, 293, 133572. https://doi.org/10.1016/j.chemosphere.2022.133572.

Andrade Pais, L. (2007). *Comportamento mecânico do solo residual granítico da Covilhã com efeito de contaminantes* [Doctoral thesis]. University of Beira Interior.

Andrade Pais, L., & Ferreira-Gomes, L. (2012). O modelo de estado crítico e o solo residual granítico: a influência do BTEX. *Revista Geotecnia*, 124(124), 31-46. https://doi.org/10.14195/2184-8394_124_2.

ASRTE SN 670. (2010). *Standard characteristic coefficients of soils.* Association of Swiss Road and Traffic Engineers Engineers, Switzerland.

ASTM D3080-04. (2004). *Standard test method for direct shear test of soils under consolidated drained conditions.* ASTM International, West Conshohocken, PA.

ASTM D420-18. (2018). *Standard guide for site characterization for engineering design and construction purposes.* ASTM International, West Conshohocken, PA.

ASTM D1883–21. (2021a). *Standard test method for California Bearing Ratio (CBR) of laboratory-compacted soils.* ASTM International, West Conshohocken, PA.

ASTM D6913/D6913M–17. (2021b). *Standard test methods for particle-size distribution (gradation) of soils using sieve analysis.* ASTM International, West Conshohocken, PA.

ASTM D698-12. (2021c). *Standard test methods for laboratory compaction characteristics of soil using standard effort (12,400 ft-lbf/ft^3 (600 kN-m/m^3)).* ASTM International, West Conshohocken, PA.

Barik, M. (2010). *Landslide susceptibility mapping to inform land use management decisions in an altered climate* [Doctoral thesis]. Washington State University. Retrieved in July 14, 2025, from https://hdl.handle.net/2376/105237

Braun, A.B., Trentin, A.W.S., Visentin, C., & Thomé, A. (2020). Sustainable remediation: a new way of thinking the contaminated sites management. *Soils and Rocks*, 43(1), 97-108. https://doi.org/10.28927/SR.431097.

Carapito, L. (2016). *Avaliação da capacidade reativa de resíduo de queima de biomassa vegetal para a remoção de cobre e zinco de efluentes líquidos* [Master thesis]. University Beira Interior.

Cheng, M., Zeng, G., Huang, D., Lai, C., Xu, P., Zhang, C., & Liu, Y. (2016). Hydroxyl radicals based advanced oxidation processes (AOPs) for remediation of soils contaminated with organic compounds: a review. *Chemical Engineering Journal*, 284, 582-598. https://doi.org/10.1016/j.cej.2015.09.001.

Chun, Y., Liu, Z., Liu, C., Zhou, D., Huang, Z., Su, J., & Liang, T. (2023). Evolution of the pore structure and permeability of thermally desorbed diesel-contaminated soils. *Acta Geotechnica*, 18(12), 6529-6557. https://doi.org/10.1007/s11440-023-01894-5.

Cunha, P. (1987). Evolução tectono-sedimentar terciária da região de Sarzedas (Portugal). *Comunicação Serviço de Geologia de Portugal*, 73(1-2), 67-84.

Dias, M.I. (1998). *Caracterização mineralógica e tecnológica de argilas especiais de bacias terciárias portuguesas* [Doctoral thesis]. University of Lisbon.

Duarte, I. (2002). *Solos residuais de rochas granitóides a sul do Tejo* [Doctoral thesis]. University of Évora.

Gomes, C.F. (1986). *Argilas: o que são e para que servem*. Lisboa: Fundação Calouste Gulbenkian.

Hewelke, E., Szatylowicz, J., Hewelke, P., Gnatowski, T., & Aghalarov, R. (2018). The impact of diesel oil pollution on the hydrophobicity and CO_2 Efflux of Forest Soils. *Water, Air, and Soil Pollution*, 229(51), 11. https://doi.org/10.1007/s11270-018-3720-6.

ISO 17892-5. (2017). *Geotechnical investigation and testing: laboratory testing of soil - part 5: incremental loading oedometer test*. International Organization for Standardization, Geneva.

ISO 17892-10. (2018a). *Geotechnical investigation and testing: laboratory testing of soil - part 10: Direct shear test*. International Organization for Standardization, Geneva.

ISO 17892-18. (2018b). *Geotechnical investigation and testing: laboratory testing of soil - part 12: Determination of liquid and plastic limits*. International Organization for Standardization, Geneva.

ISO 17892-9. (2018c). *Geotechnical investigation and testing: laboratory testing of soil - part 9: consolidated triaxial compression tests on water saturated soils*. International Organization for Standardization, Geneva.

ISO 17892-11. (2019). *Geotechnical investigation and testing - laboratory testing of soil - part 11: permeability tests*. International Organization for Standardization, Geneva.

Karkush, M., Zaboon, A., & Hussien, H. (2013). Studying the effects of contamination on the geotechnical properties. In M. Manassero (Ed.), *Coupled phenomena in environmental geotechnics* (pp. 599-607). London: Taylor & Francis Group. https://doi.org/10.1201/b15004-80.

Lemos, L., & Andrade Pais, L. (2000). Comportamento mecânico de um solo residual granítico da Covilhã. *Revista Geotecnia*, 90(90), 51-76. https://doi.org/10.14195/2184-8394_90_2.

Lv, Y., Bao, J., & Zhu, L. (2022). A comprehensive review of recent and perspective technologies and challenges for the remediation of oil-contaminated sites. *Energy Reports*, 8, 7976-7988. https://doi.org/10.1016/j.egyr.2022.06.034.

Marchiori, L., Studart, A., Albuquerque, A., Andrade Pais, L., Boscov, M.E., & Cavaleiro, V. (2022). Mechanical and chemical behaviour of water treatment sludge and soft soil mixtures for liner production. *The Open Civil Engineering Journal*, 16(1), e187414952211101. https://doi.org/10.2174/18741495-v16-e221115-2022-27.

Marchiori, L., Studart, A., Albuquerque, A., Cavaleiro, V., & Silva, A. (2021). Geotechnical characterization of water treatment sludge for liner material production and soft soil reinforcement. *Materials Science Forum*, 1046, 83-88. https://doi.org/10.4028/www.scientific.net/MSF.1046.83.

Mondelli, G., Giacheti, H.L., & Howie, J.A. (2010). Geo-environmental investigation: a brief review and a few suggestions for Brazilian contaminated sites. *Soils and Rocks*, 33(3), 171-182. https://doi.org/10.28927/SR.333171.

Ossai, I., Ahmed, A., Hassan, A., & Hamid, F. (2020). Remediation of soil and water contaminated with petroleum hydrocarbon: a review. *Environmental Technology & Innovation*, 17, 100526. https://doi.org/10.1016/j.eti.2019.100526.

Rodrigo-Ilarri, J., Rodrigo-Clavero, M.-E., Capilla, J., & Romero-Ballesteros, L. (2023). Environmental assessment of soil and groundwater pollution by BTEX leaching in Valencia Region (Spain). *Water*, 15(18), 3279. https://doi.org/10.3390/w15183279.

Roy, D., Jung, W., Kim, J., Lee, M., & Park, J. (2022). Polycyclic aromatic hydrocarbons in soil and human health risk levels for various land-use areas in Ulsan, South Korea. *Frontiers in Environmental Science*, 9, 11. https://doi.org/10.3389/fenvs.2021.744387.

Takei, T. (2019). Specific surface area. In K. Higashitani, H. Makino & S. Matsusaka (Eds.), *Powder technology handbook* (p. 5). Boca Raton: CRC Press. https://doi.org/10.1201/b22268-25.

Teixeira, G. (2009). *Geomecânica de solos em ambientes contaminados* [Master thesis]. University of Beira Interior.

Terzaghi, K., & Peck, R. (1948). *Soil mechanics in engineering practice* (11th ed.). New York: John Wiley & Sons.

United Nations. (2020). *Transforming our world: the 2030 Agenda for Sustainable Development.* Retrieved in July 14, 2025, from https://sdgs.un.org/2030agenda

Viana da Fonseca, A. (2005). *Caracterização de solos residuais em projecto geotécnico assistido por ensaios* [Doctoral thesis]. University of Porto. Retrieved in July 14, 2025, from https://hdl.handle.net/10216/67289

Yazdi, A., & Teshnizi, E. (2021). Effects of contamination with gasoline on engineering properties of fine-grained silty soils with an emphasis on the duration of exposure. *SN Applied Sciences*, 3, 704. https://doi.org/10.1007/s42452-021-04637-x.

Zhang, J., Fan, S., Yang, J., Du, X., Li, F., & Hou, H. (2014). Petroleum contamination of soil and water, and their effects on vegetables by statistically analyzing entire data set. *The Science of the Total Environment*, 476-477, 258-265. https://doi.org/10.1016/j.scitotenv.2014.01.023.

Zhao, D., Liu, C., Liu, L., Zhang, Y., Liu, Q., & Wu, W.-M. (2011). Selection of functional consortium for crude oil-contaminated soil remediation. *International Biodeterioration & Biodegradation*, 65(8), 1244-1248. https://doi.org/10.1016/j.ibiod.2011.07.008.